Front. Optoelectron. 2015, 8(1): 27–43
DOI 10.1007/s12200-014-0436-0

REVIEW ARTICLE

Semiconductor activated terahertz metamaterials

Hou-Tong CHEN (✉)

Center for Integrated Nanotechnologies, Los Alamos National Laboratory, Los Alamos, NM 87545, USA

Abstract Metamaterials have been developed as a new class of artificial effective media realizing many exotic phenomena and unique properties not normally found in nature. Metamaterials enable functionality through structure design, facilitating applications by addressing the severe material issues in the terahertz frequency range. Consequently, prototype functional terahertz devices have been demonstrated, including filters, antireflection coatings, perfect absorbers, polarization converters, and arbitrary wavefront shaping devices. Further integration of functional materials into metamaterial structures have enabled actively and dynamically switchable and frequency tunable terahertz metamaterials through the application of external stimuli. The enhanced light-matter interactions in active terahertz metamaterials may result in unprecedented control and manipulation of terahertz radiation, forming the foundation of many terahertz applications. In this paper, we review the progress during the past few years in this rapidly growing research field. We particularly focus on the design principles and realization of functionalities using single-layer and few-layer terahertz planar metamaterials, and active terahertz metamaterials through the integration of semiconductors to achieve switchable and frequency-tunable response.

Keywords terahertz, metamaterials, semiconductor, modulation

1 Introduction

The propagation of electromagnetic waves in various media is determined by the Maxwell's equations, where the electromagnetic properties of materials are described by the electric permittivity ε and magnetic permeability μ. Other electromagnetic parameters are then derived from them, such as refractive index $n^2 = \varepsilon\mu$, impedance $Z^2 = \mu/\varepsilon$, and wave vector $k^2 = \frac{\omega^2\varepsilon\mu}{c^2}$, where ω and c are the angular frequency and speed of light in vacuum, respectively. While we are familiar with the positive values of ε and μ in dielectric materials, in general they are frequency dependent complex functions, and there is no fundamental restriction that they cannot take negative values in their real part [1]. For instance, the permittivity of metals in the optical regime is negative below their plasma frequency, and the plasma frequency can be lowered to terahertz (THz) frequencies using doped semiconductors. However, except for a few ferromagnetic materials at some specific microwave frequencies, negative permeability is still not accessible using naturally existing materials at THz frequencies and beyond. The fact is that in the optical frequency regime the magnetic response is negligible, and it is quite practical to simply assume $\mu = 1$ and therefore $n = \sqrt{\varepsilon}$.

In 1999, Pendry first proposed an artificial medium exhibiting strong magnetic resonance using a periodic array of metal split-ring resonators (SRRs) [2], as shown in Fig. 1(a), where the magnetic component of the incident electromagnetic fields excites resonant circulating currents forming a magnetic dipole. When the SRRs serve as the meta-atoms and form an artificial medium, the effective magnetic permeability can be expressed in the Lorentzian form:

$$\mu_{\text{eff}} = 1 - \frac{F\omega^2}{\omega^2 - \omega_0^2 + \mathrm{i}\Gamma\omega}, \tag{1}$$

where F is the geometrical filling factor, ω_0 is the resonance frequency, and Γ is the damping rate in the lossy SRR. When the resonance is sufficiently strong, the real part of the effective permeability can take negative values over a narrow frequency range above the resonance, shown in Fig. 1(b). Together with the negative permittivity realizable using diluted plasmonic structures such as an

Received April 16, 2014; accepted June 6, 2014

E-mail: chenht@lanl.gov

This paper is dedicated to the fond memory of my friend and classmate Dr. Hua Zhong, who passed away on Dec. 8, 2013

array of metal wires [3,4], simultaneous negative permittivity and permeability were then accessible using composite media through the efforts by Smith et al. [5]. Consequently, negative refractive index metamaterials were demonstrated experimentally at microwaves [6], realizing the "substances" that Veselago speculated nearly 50 years ago [1]. In such materials, the reversal of many other electromagnetic phenomena was also predicted, but they have never been found in naturally occurring materials.

In fact, metamaterials are intelligently designed artificial media composed of subwavelength metal/dielectric structures (i.e., meta-atoms), which repeat in a periodic fashion, mimicking two or three dimensional crystalline functional

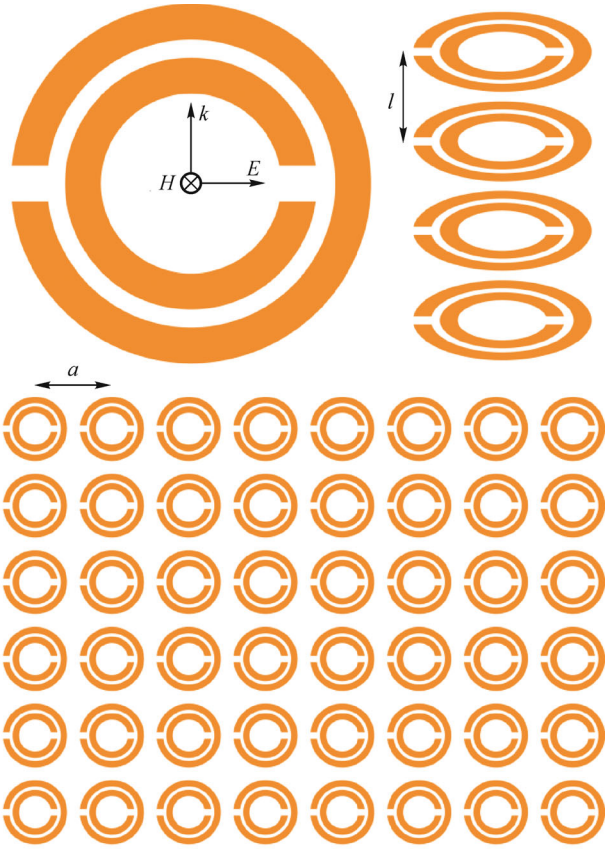

(a)

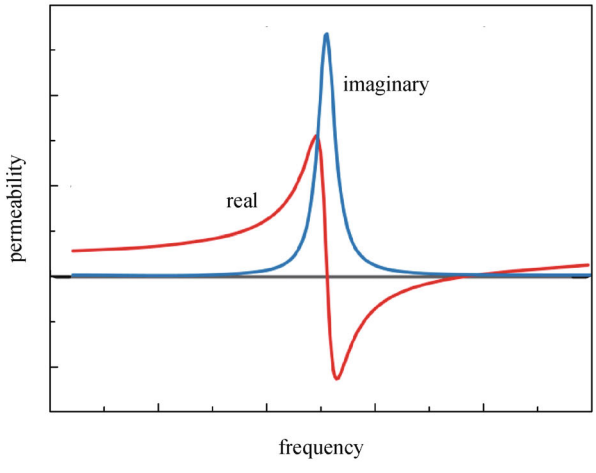

(b)

Fig. 1 (a) A metamaterial composed of a periodic array of metal split-ring resonators, where the incident magnetic field perpendicular to the metal structure can excite a resonant magnetic response, resulting in (b) a negative magnetic permeability over a narrow frequency range above the resonance. Adapted from Ref. [2]

materials. Their exotic properties are determined by the mesoscale structure rather than the composition of the materials being used and, therefore, enable electromagnetic functionality by design. One of the first inspirations that drove the research of metamaterials is the prediction of superlensing [7], which was demonstrated experimentally by Fang et al. [8]. Metamaterials allow for effective media with designed refractive index and spatial profile, which result in another excitement–transformation optics for electromagnetic invisibility [9–11]. The exotic properties realized by metamaterials have attracted ever growing worldwide interest, and consequently a variety of metamaterial structures have been developed to operate from microwave to visible regimes [12–17].

The control of electromagnetic waves lies at the core of many modern technologies, and it is critical to develop electromagnetic materials with desirable functionalities and improved performance. The realization of metamaterials seems to defy nature in their ability to produce unusual and often unexpected electromagnetic properties, providing promising opportunities and constituting a novel platform for transformative control of light propagation, light-matter interactions, and optical functionalities by rational design beyond what conventional materials can offer. Metamaterials research in the THz frequency range is driven by the special interest in solving the material issues encountered in this frequency range [18]. One of the most recent examples is that a nano-structured SRR array was demonstrated to generate coherent broadband THz pulses via nonlinear optical rectification [19]. The far-infrared or THz is considered one of the least developed frequency regimes in the electromagnetic spectrum, even though it is very attractive for numerous promising applications [20,21]. This "THz gap" is essentially due to the lack of both the classical electronic response (present for microwave and lower frequencies) and the quantum photonic response (present for infrared and higher frequencies) in the THz frequency range. It not only limits the efficient generation and sensitive detection of THz radiation, but also imposes difficulties in the effective control and manipulation of THz wave propagation including signal processing and beam steering. A designed and actively controllable resonant response, particularly in planar metamaterials, will facilitate enhanced interactions between THz radiation and functional materials, which forms the basis for the development of many THz devices and components achieving novel functionalities with unprecedented performance.

In this paper, we reviewed the progress during the past few years in this still growing research field. In Section 2, we describe the resonant response in single-layer planar metamaterials, and followed in Section 3 are the design principle and function realization using few-layer THz metamaterials. The integration of semiconductors to achieve optically switchable and frequency tunable THz metamaterials will be presented in Section 4. In Section 5, we present semiconductor hybrid metamaterials for efficient THz switching and modulation using electrical bias. We provide a brief outlook and summary in Section 6.

2 Resonant response in planar terahertz metamaterials

By scaling the geometrical dimensions of SRRs to the micrometer scale, THz metamaterials were first demonstrated by Yen et al. [12] using double SRRs. Early THz metamaterials employed relatively thick SRR structures, e.g., the metal structure thickness was 3 μm in Ref. [12] and 14 μm in Ref. [13]. Further developments showed that strong resonant response could be produced with much thinner SRRs as long as it was larger than the skin depth [22–24], which is typically in the order of 100 nm for many metals in the THz frequency range. Thicker metal SRRs resulted in marginal change in the resonance strength, but could vary the resonance frequency [25,26] and affect the sensitivity if used for sensing applications [27,28].

The fundamental resonance in a simple SRR illustrated in Fig. 2(a) can be thought of as a lumped *RLC* equivalent circuit shown in Fig. 2(b) when the incident waves are polarized along the SRR gap-bearing arm or the magnetic field is perpendicular to the SRR plane. With a steady-state the fundamental resonance frequency is given by $\omega_0 = 1/\sqrt{LC}$, where L is the loop inductance and C is the gap capacitance. When the SRR is excited by pulsed radiation, it results in a transient response and the resonant oscillation frequency is given by

$$\omega_0^2 = \frac{1}{LC} - \frac{R^2}{4L^2}, \tag{2}$$

where R represents the loss within the SRR. This has to be considered when the ohmic dissipation is significant, e.g., in superconducting metamaterials near the transition temperature [29].

In general, the response is polarization dependent, and the incident electromagnetic fields excite not only a magnetic dipole but also an electric dipole at the split gap, exhibiting bianisotropic properties. Under normal incidence (i.e., in the z direction), a planar SRR array interacts only with the electric component of the incident fields. The excited magnetic dipole does not radiate in the propagation direction, and its re-radiation in the SRR plane will be cancelled due to the subwavelength periodicity. As a result, the SRR array exhibits a pure electric response caused by the electric dipole excitation at the split gap, in contrast to the so-called "electric excitation of the magnetic resonance" [22,30,31]. In addition to the fundamental resonance, SRRs also exhibit high order resonances [32], which depend on the incidence polarization and are often very useful in designing metamaterials for multi-band operation and polarimetric applications. A planar array of

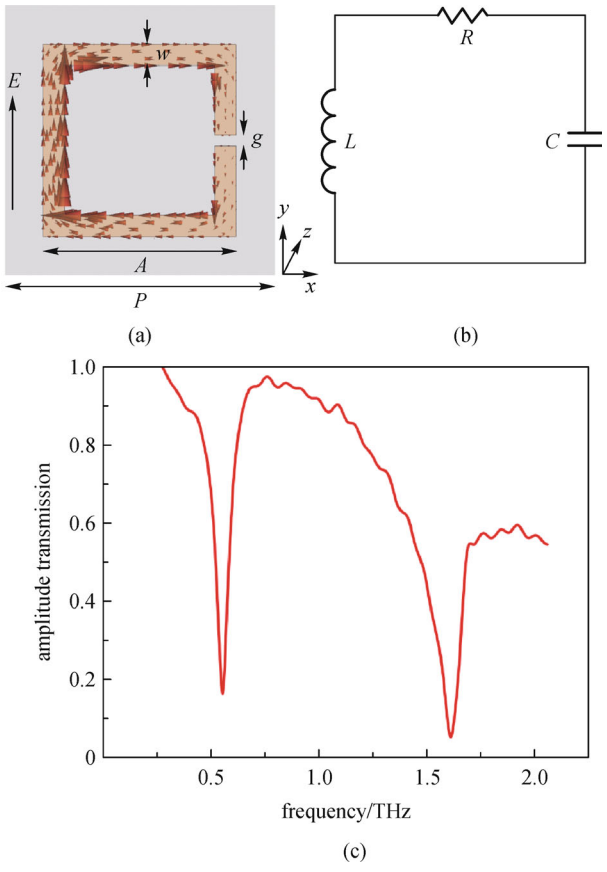

Fig. 2 (a) A simple split-ring resonator unit cell repeating in x and y directions to form a planar THz metamaterial. $P = 50$ μm, $A = 36$ μm, $w = 4$ μm, $g = 2$ μm, and the substrate is intrinsic GaAs; (b) an equivalent circuit of the split-ring resonator when the incident THz waves are polarized along the gap-bearing arm; (c) resonant transmission spectrum of the planar metamaterial normalized by the plain GaAs substrate. Adapted from Ref. [33]

SRRs is typically fabricated on a dielectric substrate (e.g., intrinsic GaAs wafers), which not only provides the necessary mechanical support but also affects the resonance frequency by introducing dielectric materials to the capacitive split gap. Figure 2(c) shows the normalized transmission spectrum of an SRR-based planar THz metamaterial under normal incidence, where the fundamental resonance is indicated by the sharp transmission dip near 0.5 THz, accompanied by a high-order resonance at 1.6 THz [33]. The magnetic resonance can only be observed under oblique incidence angles, where the magnetic field has a component perpendicular to the SRR plane [33,34].

Besides the simple SRR described above, many subwavelength resonators have been developed as the basic building block of planar metamaterials, including electric SRRs and their complements [23,35–39], asymmetric SRRs enabling Fano resonance [40,41], and many structures previously used in frequency selective surfaces [42]. The effective media theory [43] treatment using effective permittivity and permeability are meaningful for bulk metamaterials. However, single-layer planar metamaterials are better treated as effective surfaces with tuned surface impedance [44]. From a practical point of view, we may only care about the complex reflection and transmission coefficients and their dispersions, as shown in Figs. 3(c) and 3(d) for an interface between two dielectric media coated with an array of cross resonators schematically shown in Figs. 3(a) and 3(b). We can clearly see that the constant reflection and transmission coefficients now become complex functions of frequency and are strongly dispersive due to the resonance [45].

3 Functionalities in few-layer terahertz metamaterials

The strong dispersion has been thought as one of the disadvantages of metamaterials. However, one may take advantage of it to realize some promising functionalities. In addition to filtering [23], among them is the THz metamaterial perfect absorption first realized over a narrow frequency band using bi-layer metamaterials [46–48] and later evolved to an array of resonators and a metal ground plane that are separated by an ultrathin spacer [49–51]. Dual-band, multi-band and broadband THz metamaterial perfect absorbers have been demonstrated through designing the metamaterial structures exhibiting multiple resonances or using a super-unit cell consisting of different resonators [52–55]. Example structures are shown in the inset to Fig. 4(b), where the metamaterial absorbers employing a single kind of resonators operate only over a narrow bandwidth; using a super-cell consisting of resonators operating at different frequencies can expand the absorption bandwidth [56]. Although in many of the existing works the effective medium theory involving a magnetic resonance was exploited to reach the impedance matching, the perfect absorption can be conveniently explained by using an interference model [45,57] or its equivalent transmission line model [58]. The resonator array and the ground plane form a Fabry-Pérot-like resonant cavity schematically shown in Fig. 4(a), and the overall reflection is given by

$$\tilde{r} = \tilde{r}_{12} - \frac{\tilde{t}_{12}\tilde{t}_{21}\mathrm{e}^{\mathrm{i}2\tilde{\beta}_z}}{1 + \tilde{r}_{21}\mathrm{e}^{\mathrm{i}2\tilde{\beta}_z}}, \tag{3}$$

where the "~" above the variables indicate complex values, $\tilde{\beta}_z$ is the z-component of the complex propagation phase within the spacer, and the reflection coefficient of -1 at the metal ground plane has been assumed. Here the $\mathrm{e}^{-\mathrm{i}\omega t}$ sign convention has been used, and the simulated phase using CST Micwowave Studio has to be unnormalized to obtain the correct values. From the strongly dispersive reflection

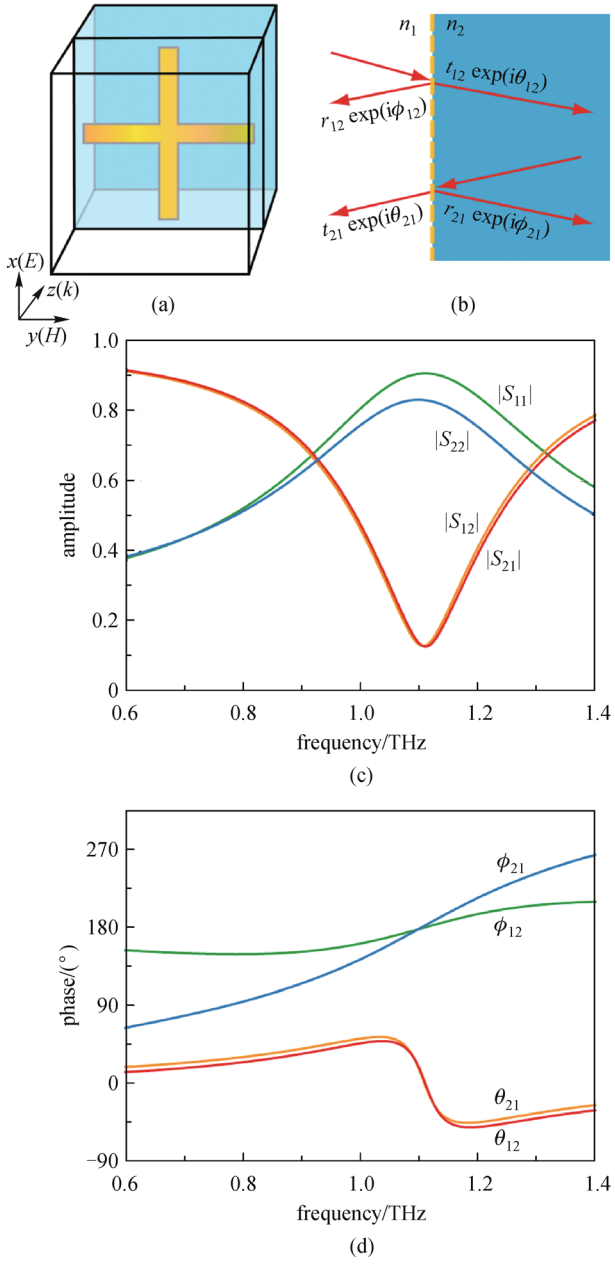

Fig. 3 (a) A unit cell of a cross resonator array at the interface between two dielectric media; (b) schematic of the reflection and transmission at the metamaterial interface; (c) amplitude and (d) phase spectra of the complex S-parameters of the metamaterial interface corresponding to the reflection and transmission coefficients under normal incidence, where $r_{12} = |S_{11}|$, $t_{12} = \sqrt{n_1/n_2}|S_{21}|$, $r_{21} = |S_{22}|$, and $t_{21} = \sqrt{n_2/n_1}|S_{12}|$. Adapted from Ref. [45]

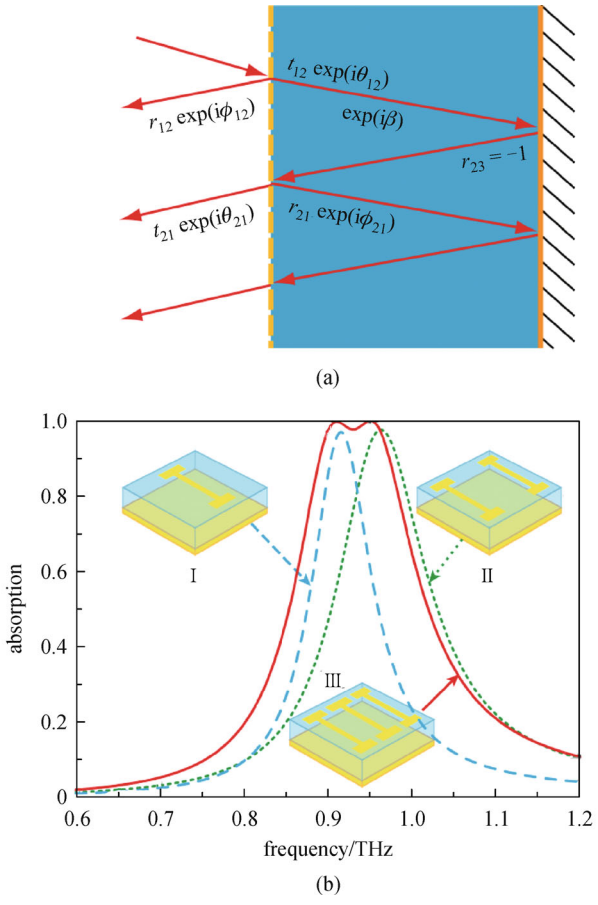

Fig. 4 (a) Schematic of multireflection within a metamaterial absorber; (b) absorption spectra under normal incidence for three metamaterial absorber configurations consisting of I-shaped resonators that are indicated in the insets. Adapted from Ref. [56]

and transmission at the metamaterial interface as shown in Figs. 3(c) and 3(d), it is possible that the multireflection destructively interferes and results in cancellation of the overall reflection when the spacer thickness (and thereby $\tilde{\beta}_z$) is carefully chosen. That is, the incident light is trapped within the metamaterial cavity until it is absorbed by the metallic structures and dielectric spacer. This theoretical model has been validated by the excellent agreement when comparing the quasi-analytical calculations, full-wave numerical simulations, and experimental measurements of many metamaterial absorber structures [45,57].

Similarly, an ultrathin planar metamaterial serving as THz antireflection coating was demonstrated using an array of resonators and a mesh separated by a low loss dielectric spacer [59,60], with the unit cell schematically shown in the inset to Fig. 5. It was shown that this ultrathin metamaterial coating is capable of dramatically reducing the reflection from a substrate surface and greatly enhancing the transmission over a narrow frequency range by design. The mechanism is the interference of the multireflection between the two metamaterial interfaces,

$$\tilde{r} = \tilde{r}_{12} + \frac{\tilde{t}_{12}\tilde{t}_{21}\tilde{r}_{23}e^{i2\tilde{\beta}_z}}{1-\tilde{r}_{21}\tilde{r}_{23}e^{i2\tilde{\beta}_z}}, \tag{4}$$

$$\tilde{t} = \frac{\tilde{t}_{12}\tilde{t}_{23}e^{i\tilde{\beta}_z}}{1-\tilde{r}_{21}\tilde{r}_{23}e^{i2\tilde{\beta}_z}}. \tag{5}$$

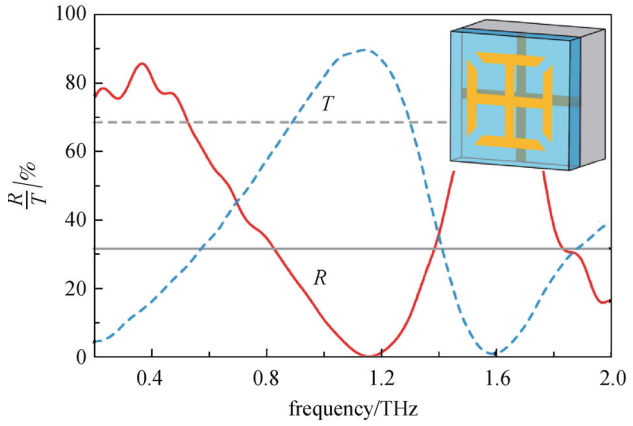

Fig. 5 Experimentally measured reflectance and transmittance under nearly normal incidence to a metamaterial coated GaAs surface. The gray horizontal lines indicate the reflectance (32%) and transmittance (68%) at a plain GaAs surface. Inset: unit cell of the metamaterial antireflection coating. Adapted from Ref. [59]

The experimental results shown in Fig. 5 are for a metamaterial coated GaAs surface, where the reflection was reduced from 32% to 0.32% and the transmission is increased from 68% to 90% near 1.2 THz. When the spacer thickness is correctly chosen, the antireflection performance is only limited by the losses of the metal and dielectric spacer being used. The metamaterial antireflection coating can operate over a wide range of incidence angle for both TE and TM polarizations. As compared to conventional antireflection coatings such as quarter-wave antireflection, this metamaterial approach is applicable to dielectric substrates with any refractive index, and there is no requirement on the refractive index of the dielectric spacer. For instance, the spacer refractive index can be even larger than the substrate refractive index. This is because the metamaterial interfaces have largely provided the required reflection/transmission amplitude and phase, and the slightly mismatched phase can be always compensated by the ultrathin spacer. Excellent agreement was obtained among the interference theory prediction, numerical simulations, and experimental results [59].

The anisotropic response in resonators that lack the 4-fold rotation symmetry could also be advantageous for polarimetric applications. Strong birefringent response can be obtained by carefully designing the resonances in the orthogonal directions. Narrowband THz waveplates were demonstrated using single-layer [61–64] and double-layer [65–67] planar metamaterials. These resonators were able to generate the cross-polarized reflection and transmission, where a phase discontinuity and gradient can be created by adjusting the geometry and dimensions, enabling anomalous reflection and refraction [68–70]. Broadband THz polarization converters (i.e., quarter and half waveplates) were also demonstrated recently using few-layer planar metamaterials, operating either in reflection or in transmission [71–73], with a linear polarization rotator shown in Fig. 6. It was shown that the interference associated with the multi-layer structures played an essential role [71]. Using a variety of resonator geometries and dimensions, a phase gradient could be created for high efficiency arbitrary wavefront shaping such as flat THz prisms [71] and lenses [74,75].

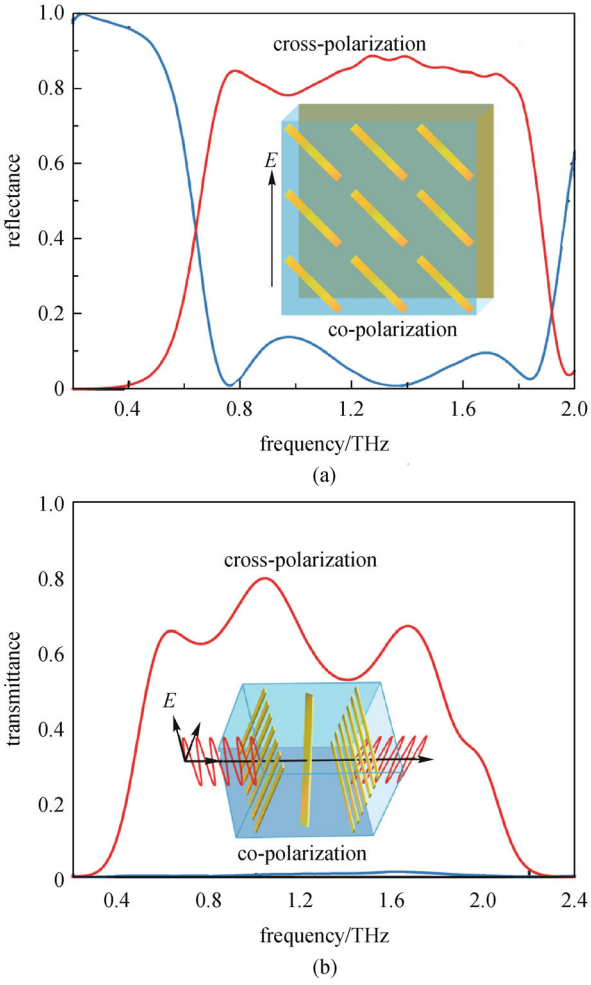

Fig. 6 Experimental results of broadband THz linear polarization rotators in reflection (a) and transmission (b). Adapted from Ref. [71]

In realizing all of the abovementioned THz functionalities, the resonant response and the strong dispersion in planar metamaterials play the essential role. So far almost all THz metamaterials exploited single-layer or few-layer planar structures, as fabrication of three-dimensional metamaterials with micrometer feature sizes is technically challenging [76–80]. Such designs may also alleviate high losses associated with the resonant response in bulk metamaterials. Just as in modern semiconductor industry where device architectures suitable for planar fabrication processes were eventually employed to build very large scale integrated electronic circuits, it is of utmost importance to investigate and discover novel functional-

ities in planar metamaterials toward practical applications. Besides the passive functionalities described above, it is highly desirable to realize active, controllable, and nonlinear metamaterials through integrating active functional materials to obtain enhanced functionalities.

4 Optically tunable terahertz metamaterials

As described in the previous sections, the functionalities of metamaterials critically depend on the resonance and, in case of few-layer metamaterials, the spacer thickness and material properties. Metamaterial resonators can be equivalent to resonant *RLC* circuits and therefore the task of realizing actively switchable and frequency tunable metamaterials is how to integrate functional materials forming hybrid metamaterials to modify the resistance R (resonance damping), capacitance C and inductance L (resonance frequency), and spacer properties using external stimuli such as temperature, optical excitation, voltage bias, and magnetic field. Semiconductors become the materials of choice due to the developed device physics and matured integration and fabrication technology. Intrinsic semiconductors have very low conductivity as in dielectrics, so they can be used as the metamaterial substrate to enable strong resonances. The conductivity can be increased by orders of magnitude through doping enabling metallic behavior. Furthermore, active modification of the conductivity can be realized by carrier injection and depletion through photoexcitation and voltage bias. Such a unique capability makes semiconductors ideal to be integrated into metamaterial structures to accomplish active and dynamical functionalities. In designing hybrid THz metamaterials through numerical simulations, the Drude model can be used for the dielectric function of the integrated semiconductors:

$$\varepsilon(\omega) = \varepsilon_\infty - \frac{\omega_p^2}{\omega^2 + i\omega\gamma}, \tag{6}$$

where ε_∞ is the high frequency permittivity, γ is the damping rate, and ω_p is the plasma frequency related to the electron density n, effect electron mass m^*, and electron charge e as

$$\omega_p^2 = \frac{ne^2}{\varepsilon_0 m^*}. \tag{7}$$

The parameters ω_p and γ can be obtained by experimental measurements.

The first dynamical THz metamaterial was demonstrated in 2006 by Padilla et al., where a planar array of SRRs was fabricated on top of an intrinsic GaAs substrate [33], see Fig. 2(a). As shown in Fig. 7, the strong fundamental resonance is completely switched off through near-infrared femtosecond laser excitation of electron-hole pairs in the substrate surface at a fluence of about 2 μJ/cm^2 (corresponding to 1 mW), equivalent to a free charge carrier density of about 4×10^{16} cm^{-3}. Correspondingly, the normalized resonant field transmission at 0.56 THz increased from 15% to 70%. This can be understood that the created charge carriers upon photoexcitation in the semiconducting substrate, particularly within the split gap of SRRs, provide strong damping to the resonance. In other words, the SRRs are short-circuited and the resonance is switched off.

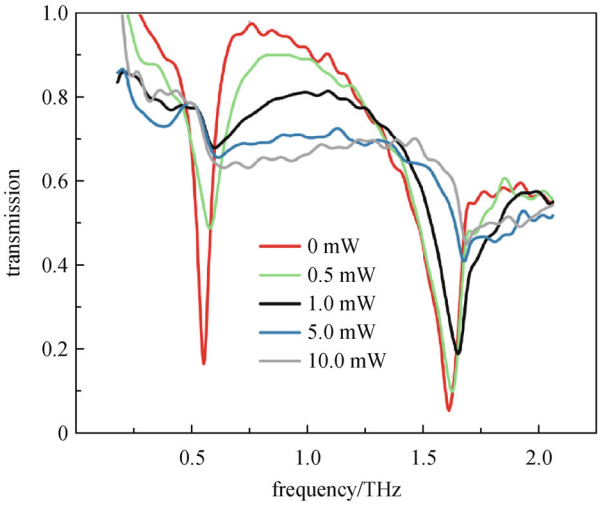

Fig. 7 THz transmission spectra of a planar split-ring resonator array fabricated on top of an intrinsic GaAs substrate under near-infrared femtosecond laser excitation with various powers. Adapted from Ref. [33]

The carrier lifetime in GaAs substrate is in the order of nanosecond, which limits the switching recovery. To accomplish ultrafast switching of the metamaterial resonances, other semiconductors or semiconducting structures are needed, e.g., radiation damaged silicon, low temperature grown GaAs, and ErAs/GaAs nanoisland superlattices. Particularly, the carrier lifetime in ErAs/GaAs superlattices can be controlled during the MBE growth by engineering the superlattice periodicity, ranging from subpicosecond to tens of picoseconds [81], which is ideal to realize ultrafast switching speed of THz radiation. When arrays of electric SRRs and the complementary structures were fabricated on ErAs/GaAs superlattice substrates with carrier lifetime about 10 ps, Chen et al. demonstrated ~20 ps switching recovery time [82]. At the resonance frequency of 0.73 THz, the normalized field transmission recovered within 20 ps from 36% to 17% and from 7.5% to 29%, respectively, for the original and complementary arrays of electric SRRs.

Upon photoexcitation, the semiconducting substrates themselves can switch and modulate the transmission of THz radiation. The advantage of combining semiconductors with THz metamaterials is that the resonance

concentrates the incident THz field at particular regions, e.g., split gap of SRRs, and therefore dramatically magnifies the switching and modulation. As such, it can significantly reduce the required fluence of optical excitation to reach comparable or exceeding performance. This becomes manifest when semiconductors are integrated only at the split gaps of an SRR array rather than serving as the substrate [83], as shown in Fig. 8(a). In the absence of photoexcitation the metamaterial exhibits two strong resonances at 0.6 THz (first order) and 1.75 THz (third order); upon photoexcitation the metamaterial shows only one resonance at 1.3 THz (second order) as if in a closed ring resonator, shown in Figs. 8(b) and 8(c). Following this consideration it is possible to achieve ultra broadband THz modulation, for instance, using metal-to-insulate transition in metallic structures [84].

When two SRRs are arranged face-to-face as illustrated in the inset to Fig. 9, the excited electric dipoles at the split gaps will cancel each other and exhibit sub-radiative properties (i.e., dark mode). The SRR pair can couple with a super-radiative cut-wire dipole resonator (i.e., bright mode), which was used to realize the classical analog of electromagnetically induced transparency (EIT) in the THz regime [85]. The interference between the bright and dark modes results in a transparency window indicated by the sharp transmission peak at 0.74 THz between the two transmission dips, shown in Fig. 9. Upon photoexcitation, the integrated silicon pads at the split gaps become conducting and shunt the resonance of the SRRs. Therefore, only the dipole resonance from the cut-wire array remains and the THz transmission spectrum reveals only one transmission dip. Such a giant switching of EIT is accompanied with an actively controllable group delay of the THz waves, potentially in an ultrafast time scale, e.g., using radiation damaged silicon that has been used to investigate the ultrafast manipulation of near field coupling between SRRs in THz metamaterials [86].

It was also shown that integrating semiconductors as a part of the metamaterial resonators can tune the metamaterial resonance frequency over a large frequency range. This was first demonstrated by using an array of electric SRRs fabricated on a sapphire substrate, where two high-resistivity silicon strips were integrated at the split gap of the SRRs [87], shown in Figs. 10(a) and 10(b). Upon optical excitation, the two silicon strips become highly conducting and form capacitive plates, resulting in an increase in capacitance and a red-shifting of metamaterial resonance from 1.06 to 0.85 THz, a change of over 20% in experiments. Numerical simulations also revealed that blue-shifting was possible when semiconductor strips form parts of the SRR current loops by reducing the overall inductance after photoexcitation. Shen et al. revised the metamaterial designs using an electric SRR variant unit cell with multiple loops and split gaps and incorporated silicon islands filling one set of the gaps [88,89]. After photoexcitation, the loops associated with the gaps filled

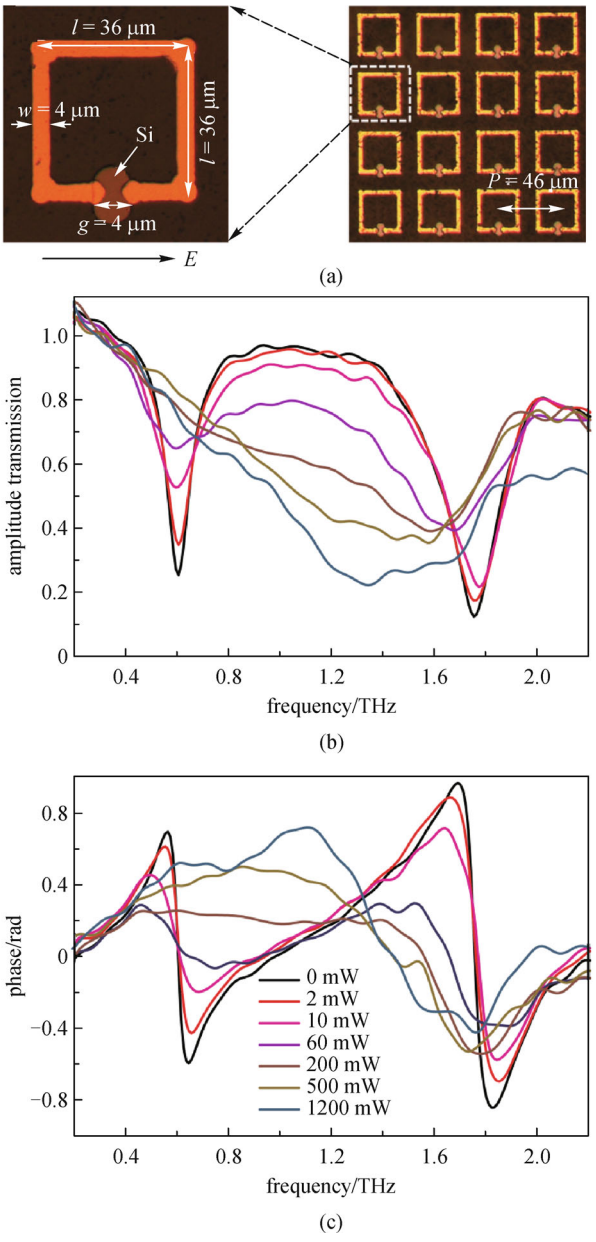

Fig. 8 (a) Optical microscopy images of the split-ring resonator array with silicon pads integrated at the split gaps; (b) THz transmission amplitude and (c) phase spectra under various powers of near-infrared femtosecond laser excitation. Adapted from Ref. [83]

with silicon are short-circuited, which modifies the resonance resulting in a blue-shifting of the metamaterial resonance from 0.76 to 0.96 THz, a change of 26% observed in experiments.

These dynamical metamaterials can be classified into two categories: 1) the semiconductor fills the split gaps (including serving as the substrate) of the metamaterial resonators for resonance damping, and 2) the semiconducting material is part of the metamaterial resonator for frequency tuning. A combination of these two approaches

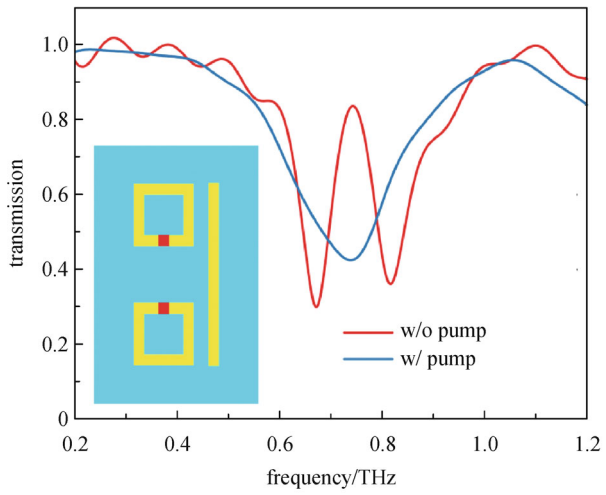

Fig. 9 Experimentally measured transmission spectra of the THz EIT metamaterial (unit cell shown in the inset) without (red curve) and with (blue curve) photoexcitation. Adapted from Ref. [85]

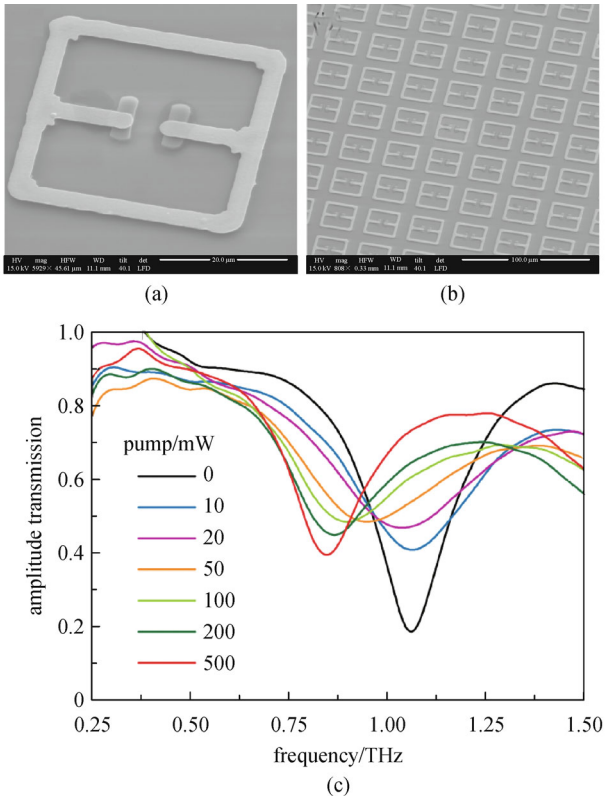

Fig. 10 Scanning electron microscopy images of (a) an individual unit cell and (b) a square array of electric split-ring resonators where silicon strips were incorporated at the split gap; (c) experimentally measured THz transmission spectra at various photoexcitation power levels. Adapted from Ref. [87]

was used by Zhang et al. to realize handedness switching in THz chiral metamaterials [90]. The THz chiral metamaterial design is based on a vertical metallic chiral resonator, in which the chirality is introduced by tilting the loop of the resonator out of the plane with its gap [91]. Two such meta-atoms with mirror symmetry (and therefore opposite chirality) are put together forming the metamolecule as shown in Fig. 11(a) and showing no chirality. When a small part of the metal structure in one meta-atom is replaced with a silicon pad, the chiral resonance frequency increases from ω_0 to ω_1; while in the other meta-atom a silicon pad is introduced to link the metal structure, keeping its opposite chiral resonance frequency at ω_0 in the absence of photoexcitation, as shown in Fig. 11(b). The resulted meta-molecule then shows left-handed chiral resonance at ω_0, and right-handed chiral resonance at ω_1. Upon photoexcitation the silicon regions become highly conducting, the first meta-atom increases its geometric dimension and lowers its chiral resonance frequency from ω_1 back to ω_0, and the resonance in the other meta-atom at ω_0 is completely damped. The overall effect is the optoelectronic switching of the electromagnetic chirality, as shown in Fig. 11(c) for the reversed circular dichroism, which was also experimentally observed [90]. Another dynamical chiral THz metamaterial consisting of an array of conjugated bilayer metal structures with additional silicon integration was also demonstrated with giant and dynamically tunable optical activity [92].

In some applications, the substrate of an active metamaterial is not desirable and needs to be removed. For the few-layer metamaterials presented in Section 3, the growth of high quality epitaxial film is not feasible. In such cases, the integration of semiconductor materials requires a film transfer process. Fan et al. fabricated electric SRRs on epitaxial GaAs film patches, which was on top of an $Al_{0.95}Ga_{0.05}As$ layer that can be etched later. A polyimide film was spun on top of the metamaterial so that after etching the $Al_{0.95}Ga_{0.05}As$ layer the SRRs together with the GaAs patches were released and attached on the polyimide, forming a flexible free-standing active THz metamaterial [93]. The optical switching of the metamaterial resonance was characterized by using optical-pump THz-probe experiments, agreeing well with the numerical simulations. This approach opens a way of integrating semiconducting functional materials into few-layer metamaterials to accomplish active THz functionalities.

5 Electrically switchable terahertz metamaterials and terahertz modulation

Semiconducting hybrid metamaterials also feature electrical tuning of resonances via application of a voltage bias. The first electrically switchable THz metamaterial device was demonstrated by Chen et al. through fabricating an array of electric SRRs on top of a 1 μm thick *n*-doped epitaxial GaAs layer grown on an intrinsic GaAs substrate [94], as schematically shown in Fig. 12(a). The electric SRR array was designed to have two resonances at 0.72

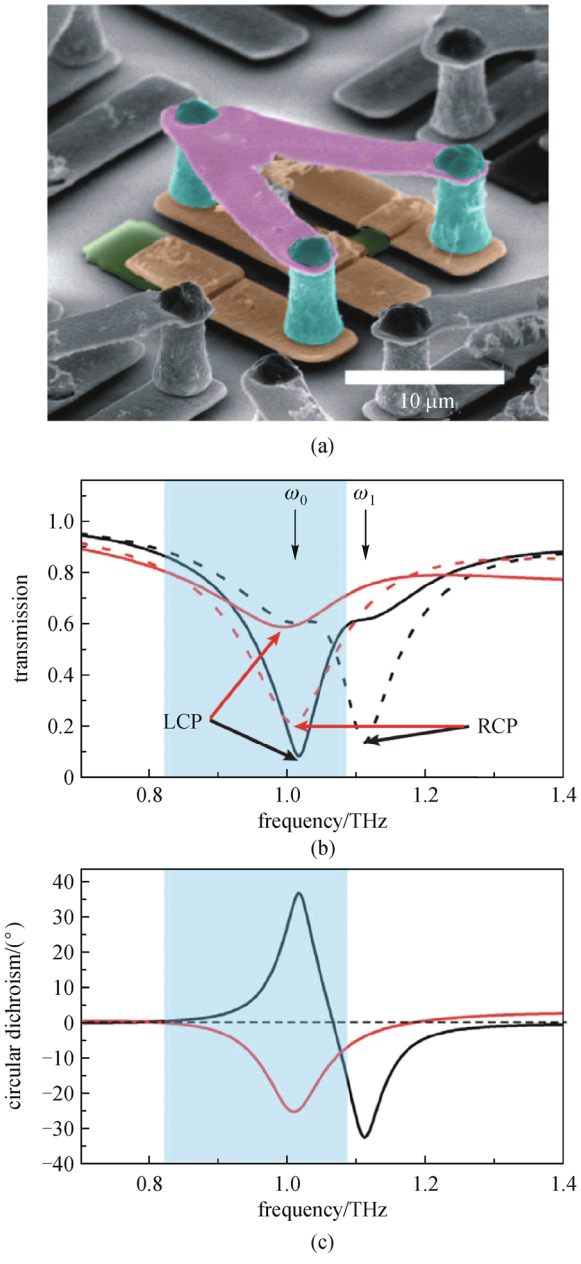

Fig. 11 (a) Scanning electron microscopy image of the dynamically switchable chiral meta-molecule; (b) simulated transmission spectra of left (solid curves) and right (dashed curves) handed circular polarizations before (black curves) and after (red curves) near-infrared photoexcitation; (c) circular dichroism before (black curve) and after (red curve) photoexcitation. Adapted from Ref. [90]

and 1.66 THz, and the resonant elements were interconnected, which did not affect the resonances because of the symmetric structure when the polarization of the incident THz radiation was perpendicular to the connecting wires. The metallic metamaterial structure forms a Schottky gate to the *n*-doped GaAs creating a depletion region known as Schottky junction, where the carrier density can be controlled via the application of a reverse voltage bias. In the absence of a voltage bias, the depletion region is narrow and the split gap of the eSRRs is effectively shunted by the conducting substrate. The resonances are almost completely damped, resulting in relatively flat transmission characteristics. A reverse voltage bias depletes the charge carriers in the substrate near the metallic structures, which modifies the gap from conducting to insulating, and thereby recovers the metamaterial resonant response, as shown in Fig. 12(b). It was shown that, upon a reverse voltage bias of −16 V, both resonances were switched, with power transmission decreases from 45% to 22%, a modulation depth of 50% at 0.72 THz, and from 17% to 4%, a modulation depth of 76% at 1.65 THz, though the latter exhibits higher insertion loss. At frequencies between the two resonances, the transmission increases, from 48% to 86% at 0.94 THz.

The THz modulation can be further improved through optimizing the resonator structure. In another demonstration, the power modulation depth at the fundamental resonance (0.81 THz) was increased to 80% [95], as shown in Fig. 13(a). The electrical switching of the metamaterial resonances yet yielded additional functionality–phase control of the THz radiation shown in Fig. 13(b) [95]. For transmission, there is no phase change at resonance where the transmission amplitude changes the most, indicated by the vertical dashed lines in Fig. 13. While at the frequency where the transmission amplitude keeps largely constant, the phase experiences significant shift, indicated by the vertical solid line. At the off-resonance frequency of 0.89 THz, the transmission amplitude has negligible change upon a voltage bias of −16 V, but the phase decreases from 0.05 to −0.51 rad, a change of 0.56 rad, or 50π per wavelength when considering the effective physical thickness 1.2 μm of the device.

In general, the frequency dependent transmission coefficient is complex and contains the amplitude and phase information, both of which contribute to the THz modulation through

$$|\Delta\tilde{t}(\omega)| = \left| t_{V_1}(\omega)\mathrm{e}^{\mathrm{i}\varphi_{V_1}(\omega)} - t_{V_2}(\omega)\mathrm{e}^{\mathrm{i}\varphi_{V_2}(\omega)} \right|, \qquad (8)$$

where V_1 and V_2 indicate the minimum and maximum values of the alternating voltage bias. It turns out that although the metamaterial resonances are narrowband, the correlated amplitude switching and phase shifting shown in Fig. 13 results in the demonstration of a broadband (0.7–1.7 THz) electrical THz modulator through the application of an ac voltage bias alternating between 0 and –16 V, shown in Fig. 13(c). The device was used to replace the mechanical optical chopper in the THz time-domain spectroscopy system with modulation speed increased to a few tens of kHz [95].

The modulation speed of the electrically driven THz metamaterial modulators is limited by the *RC* time constant. In the aforementioned devices, the device resistance is ~100 Ω, while the capacitance is determined

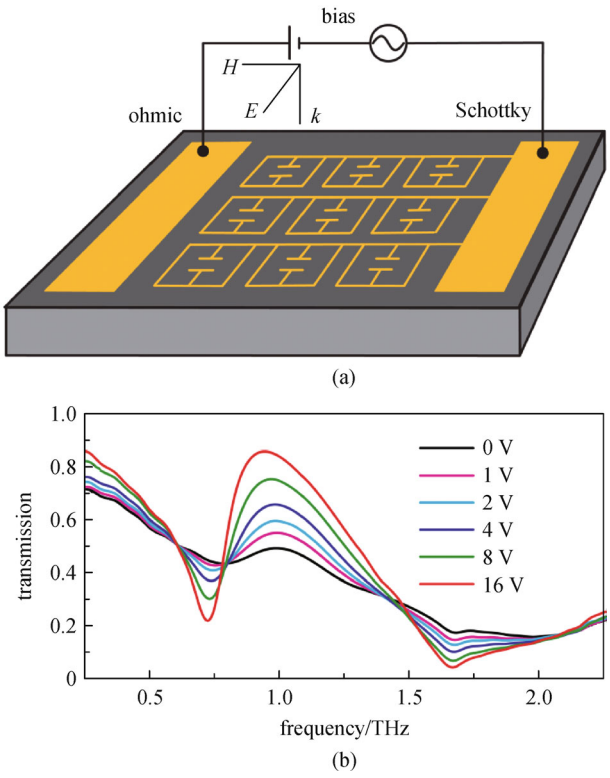

Fig. 12 (a) Design schematic of electrically switchable THz metamaterial, which is an array of interconnected electric split-ring resonators fabricated on top of a thin layer of *n*-doped GaAs substrate; (b) THz transmission spectra (intensity) as a function of the applied reverse voltage bias. Adapted from Ref. [94]

by the device area. The large device area (5 mm × 5 mm) in addition to the large Schottky electrical pad (2 mm × 5 mm) results in high value of capacitance, and therefore the modulation speed is limited to ~100 kHz. Reducing the device area as well as using minimal size of the Schottky electrical pad, a modulation speed of 2 MHz was demonstrated [96]. Shrekenhamer et al. integrated high electron mobility transistors (HEMTs) into the split gaps of electric SRRs (see Fig. 14) and realized modulation speed ~10 MHz with a decent modulation depth (field amplitude modulation 33%) at ~0.46 THz [97]. The modulation speed may be further increased by reducing the parasitic capacitance through metamaterial structure optimization.

The implementation of electrically controllable Schottky depletion was also used to switch the resonant response of surface plasmon polaritons, where periodic metallic hole arrays were fabricated on top of doped GaAs substrate [98]. The switching of the extraordinary light transmission exhibited similar modulation depth at the resonance frequencies. However, they also showed higher insertion losses and narrowband operation. While many of electrically switchable THz metamaterial devices are polarization sensitive due to the use of resonant element lacking 4-fold rotation symmetry and the implementation of

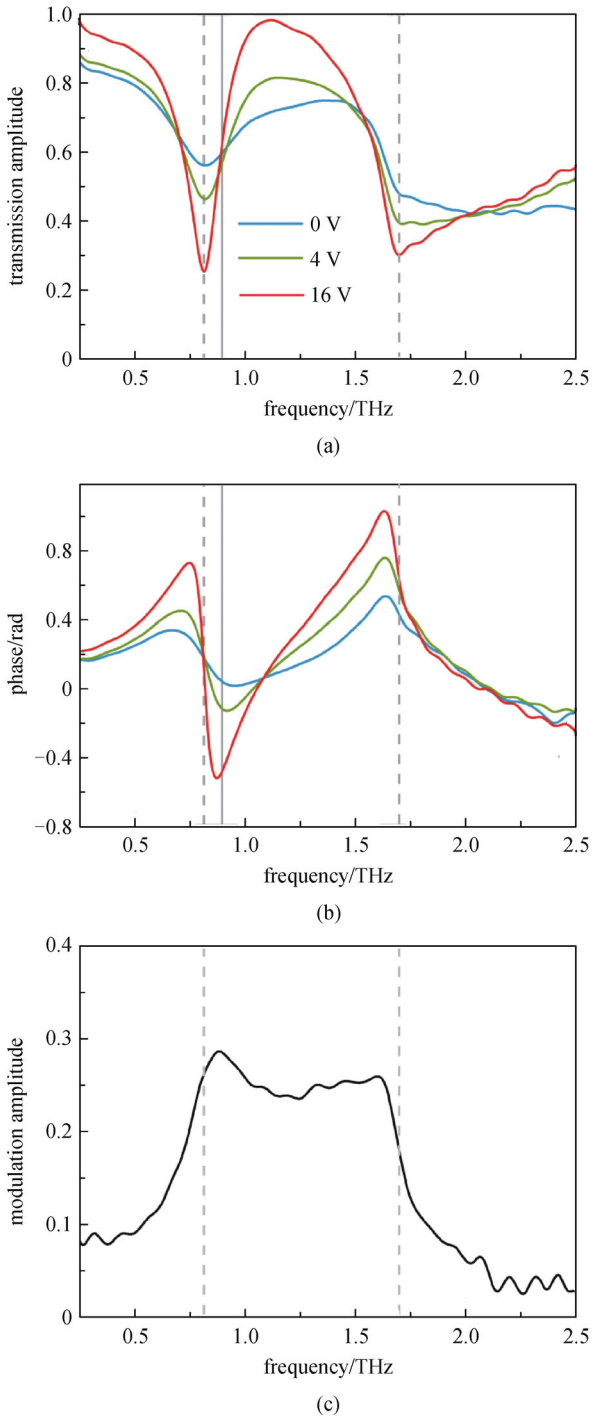

Fig. 13 Correlated transmission amplitude (a) and phase (b) spectra under various reverse voltage biases to an electrically switchable THz metamaterial; (c) THz modulation signal normalized to the incident THz spectrum under a square electrical signal alternating between 0 and −16 V. Adapted from Ref. [95]

connecting wires, Paul et al. demonstrated a polarization independent device through a more symmetric design of resonators (cross resonators) and using very narrow connecting wires in the two orthogonal directions [99].

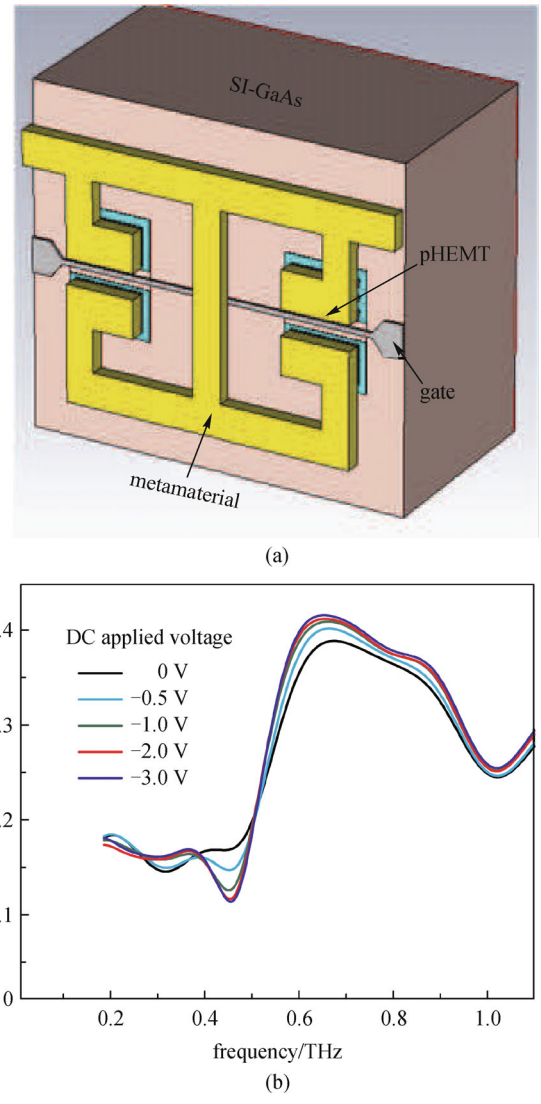

Fig. 14 (a) Schematic of the single unit cell of HEMT based electronically controllable THz metamaterial modulator, where the HEMT is identified and lies under each split gap of the metamaterial; (b) frequency dependent transmitted THz electric field for the HEMT/metamaterial device as a function of voltage bias. Adapted from Ref. [97]

For the THz metamaterial modulation devices based on Schottky depletion, there is also a trade-off between the operation frequency and depletion depth. One has to increase the doping and thereby increase the plasma frequency in order to sufficiently damp the metamaterial resonance when the device is designed to operate at higher frequencies. However, the depletion depth is significantly reduced with higher doping, limiting the re-establishment of the resonance. Electrically-driven active metamaterials were demonstrated to externally modulate THz quantum cascade lasers (QCLs) operating at 2.4 and 2.8 THz, obtaining a maximum modulation depth of ~60% [100]. The operation seems to be dominated by the resonance shifting due to the depletion of the doped substrate, which causes a change of the substrate dielectric constant and resonance frequency, in contrast to the resonance damping as previously shown.

The excellent modulation depth, extended bandwidth, and relatively high modulation speed make the THz metamaterial modulator ideal for applications such as spatial light modulation for THz imaging. A THz spatial light modulator (SLM) consisting of 4 × 4 pixels was demonstrated by Chan et al., where each pixel was independently switched by an external voltage bias and was a 4 mm × 4 mm array of eSRRs designed to resonate at 0.36 THz [101]. The experimental results showed negligible cross-talk among pixels, and diffraction patterns were observed in experiments when these pixels were switched to form columns as diffraction slits. Another THz SLM based on active THz metamaterial absorber was demonstrated by Shrekenhamer et al. [102]. It consists of 4 × 4 superpixels, each of which has 4 pixels operating at different frequencies. The experimental demonstration reveals an average modulation depth of 62% and switching speed up to 12 MHz. These high-speed metamaterial SLMs are very attractive for single-pixel THz imaging applications.

Along the pixelization consideration, a new scheme of THz modulation was then proposed and demonstrated based on electrically switchable metamaterials diffraction grating shown in Fig. 15 [103]. This takes advantage of the fact that the resonant elements can be grouped into independent columns, which can be engineered into grating patterns with independent electrical control. The application of appropriate voltage bias to these columns switches the metamaterial structure between uniform and grating. This allows the modulation of the diffraction beam, which is in principle background-free and therefore enables a very high modulation depth, in the spirit of a conventional acousto-optic modulator. Off-axis diffraction was observed over a wide frequency band due to the correlated amplitude and phase modulation, and more than 20 dB of dynamical range was obtained as shown in Fig. 16, a THz modulation depth exceeding the current state-of-the-art. Tailoring the metamaterial resonances and pixelization offered a powerful strategy for the development of THz devices with greatly improved performance for many applications.

6 Outlook and summary

It is clear that the limited electromagnetic and photonic response available in naturally occurring materials is insufficient for emerging technologies with increasing demanding requirements. To address the challenges in developing next generation optoelectronic and photonic technologies, it is critical to create novel materials with desirable functionalities and improved performance. The ability of control the electromagnetic response by design of

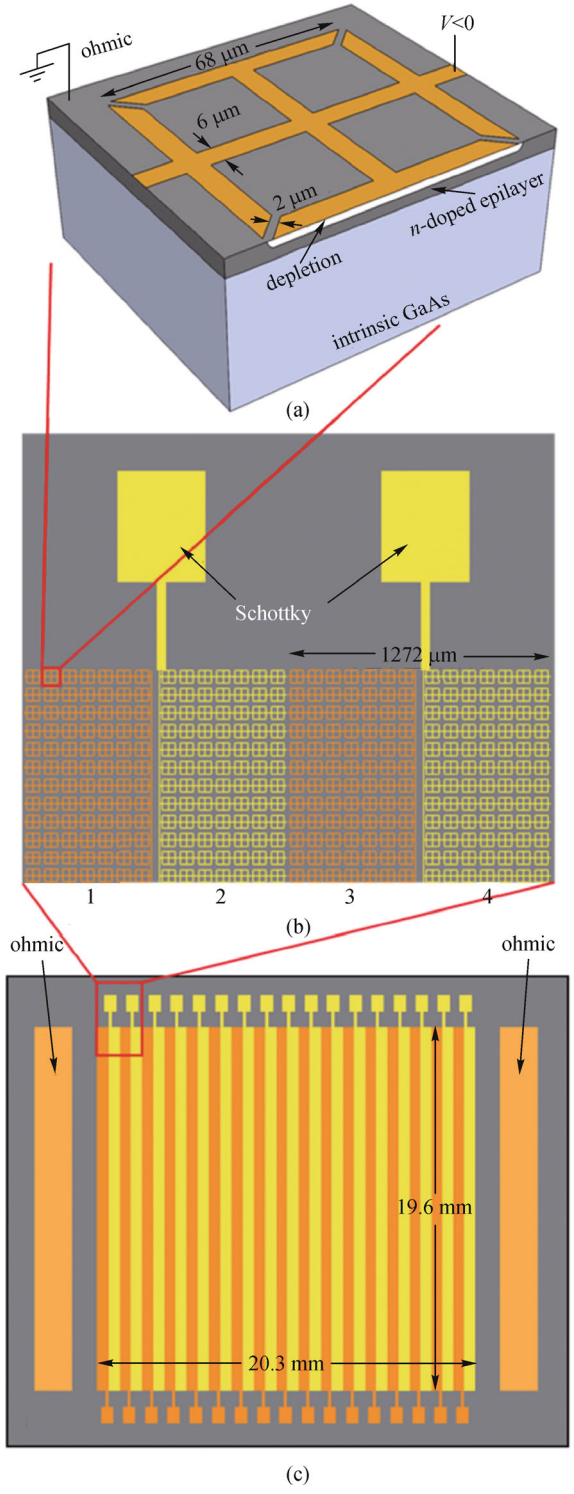

Fig. 15 A unit cell illustrating an electric split-ring resonator array fabricated on top of the *n*-doped GaAs epilayer in the reverse biased state; (b) schematic showing a portion of the first four grating strips formed by interconnected electric split-ring resonators; (c) illustration of the entire metamaterial grating. The color profile illustrates that alternate columns are biased forming a diffraction grating, with each column being independently controlled by the voltage bias between its Schottky pads and the ohmic contacts. Adapted from Ref. [103]

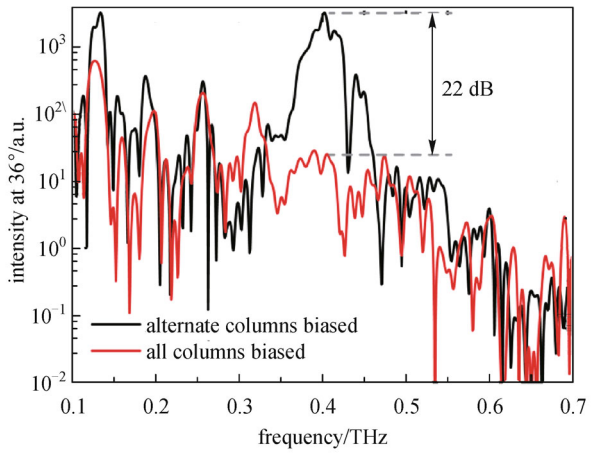

Fig. 16 Intensity spectra of the differential diffracted signal at the off-axis angle of 36° when applying an alternating voltage bias at 1 kHz to the device shown in Fig. 14. Adapted from Ref. [103]

materials is certainly a dream for scientists and engineers. The development of metamaterials provides such a promising opportunity and makes this dream become a reality, particularly in solving the material issues encountered in the THz frequency range. In this paper, we have shown examples of THz functionalities through metamaterial structure design, which may be only limited by our imagination and creativity. The resonant response in metamaterials enables enhanced light-matter interactions with the integration of additional functional materials. This forms the basis for advanced functionalities such as THz modulation that is necessary in almost any applications.

The research of metamaterials is one of the most rapidly developing fields. Even in this paper we focus on the semiconductor activated THz metamaterials, there are many other developments involving semiconductor hybrid THz metamaterials that we have not included, for instance, enhanced nonlinear response [104] and ultrastrong light-matter interactions [105]. Besides semiconductors, many other functional materials such as graphene, semiconducting quantum wells, complex metal oxides, superconductors, and liquid crystals, can be integrated, where the few-layer planar metamaterials may provide novel device architectures, revolutionizing the next generation devices. These hybrid metamaterials may not only enable enhanced active functionalities in the THz frequency range, but also have the potential to realize many photonic and optoelectronic applications in the optical frequency regimes.

Acknowledgements We acknowledge partial support from the Los Alamos National Laboratory Laboratory-Directed Research and Development program. This work was performed in part at the Center for Integrated Nanotechnologies, a US Department of Energy, Office of Basic Energy Sciences user facility. Los Alamos National Laboratory, an affirmative action equal opportunity employer, is operated by Los Alamos National Security for the National Nuclear Security Administration of the US Department of Energy under contract DE-AC52-06NA25396.

References

1. Veselago V G. The electrodynamics of substances with simultaneously negative values of ε and μ. Soviet Physics Uspekhi-USSR, 1968, 10(4): 509–514
2. Pendry J B, Holden A J, Robbins D J, Stewart W J. Magnetism from conductors and enhanced nonlinear phenomena. IEEE Transactions on Microwave Theory and Techniques, 1999, 47 (11): 2075–2084
3. Pendry J B, Holden A J, Stewart W J, Youngs I. Extremely low frequency plasmons in metallic mesostructures. Physical Review Letters, 1996, 76(25): 4773–4776
4. Wu D M, Fang N, Sun C, Zhang X, Padilla W J, Basov D N, Smith D R, Schultz S. Terahertz plasmonic high pass filter. Applied Physics Letters, 2003, 83(1): 201–203
5. Smith D R, Padilla W J, Vier D C, Nemat-Nasser S C, Schultz S. Composite medium with simultaneously negative permeability and permittivity. Physical Review Letters, 2000, 84(18): 4184–4187
6. Shelby R A, Smith D R, Schultz S. Experimental verification of a negative index of refraction. Science, 2001, 292(5514): 77–79
7. Pendry J B. Negative refraction makes a perfect lens. Physical Review Letters, 2000, 85(18): 3966–3969
8. Fang N, Lee H, Sun C, Zhang X. Sub-diffraction-limited optical imaging with a silver superlens. Science, 2005, 308(5721): 534–537
9. Pendry J B, Schurig D, Smith D R. Controlling electromagnetic fields. Science, 2006, 312(5781): 1780–1782
10. Leonhardt U. Optical conformal mapping. Science, 2006, 312 (5781): 1777–1780
11. Schurig D, Mock J J, Justice B J, Cummer S A, Pendry J B, Starr A F, Smith D R. Metamaterial electromagnetic cloak at microwave frequencies. Science, 2006, 314(5801): 977–980
12. Yen T J, Padilla W J, Fang N, Vier D C, Smith D R, Pendry J B, Basov D N, Zhang X. Terahertz magnetic response from artificial materials. Science, 2004, 303(5663): 1494–1496
13. Moser H O, Casse B D F, Wilhelmi O, Saw B T. Terahertz response of a microfabricated rod-split-ring-resonator electromagnetic metamaterial. Physical Review Letters, 2005, 94(6): 063901
14. Linden S, Enkrich C, Wegener M, Zhou J, Koschny T, Soukoulis C M. Magnetic response of metamaterials at 100 terahertz. Science, 2004, 306(5700): 1351–1353
15. Shalaev V M, Cai W, Chettiar U K, Yuan H K, Sarychev A K, Drachev V P, Kildishev A V. Negative index of refraction in optical metamaterials. Optics Letters, 2005, 30(24): 3356–3358
16. Zhang S, Fan W, Panoiu N C, Malloy K J, Osgood R M, Brueck S R J. Experimental demonstration of near-infrared negative-index metamaterials. Physical Review Letters, 2005, 95(13): 137404
17. Enkrich C, Wegener M, Linden S, Burger S, Zschiedrich L, Schmidt F, Zhou J F, Koschny T, Soukoulis C M. Magnetic metamaterials at telecommunication and visible frequencies. Physical Review Letters, 2005, 95(20): 203901
18. Chen H T, O'Hara J F, Azad A K, Taylor A J. Manipulation of terahertz radiation using metamaterials. Laser & Photonics Reviews, 2011, 5(4): 513–533
19. Luo L, Chatzakis I, Wang J, Niesler F B P, Wegener M, Koschny T, Soukoulis C M. Broadband terahertz generation from metamaterials. Nature Communications, 2014, 5: 3055
20. Ferguson B, Zhang X C. Materials for terahertz science and technology. Nature Materials, 2002, 1(1): 26–33
21. Tonouchi M. Cutting-edge terahertz technology. Nature Photonics, 2007, 1(2): 97–105
22. Azad A K, Dai J, Zhang W. Transmission properties of terahertz pulses through subwavelength double split-ring resonators. Optics Letters, 2006, 31(5): 634–636
23. Chen H T, O'Hara J F, Taylor A J, Averitt R D, Highstrete C, Lee M, Padilla W J. Complementary planar terahertz metamaterials. Optics Express, 2007, 15(3): 1084–1095
24. Singh R, Smirnova E, Taylor A J, O'Hara J F, Zhang W. Optically thin terahertz metamaterials. Optics Express, 2008, 16(9): 6537–6543
25. Chiam S Y, Singh R, Gu J Q, Han J G, Zhang W L, Bettiol A A. Increased frequency shifts in high aspect ratio terahertz split ring resonators. Applied Physics Letters, 2009, 94(6): 064102
26. Chiam S Y, Singh R, Zhang W L, Bettiol A A. Controlling metamaterial resonances via dielectric and aspect ratio effects. Applied Physics Letters, 2010, 97(19): 191906
27. O'Hara J F, Singh R, Brener I, Smirnova, Han J, TaylorA J, Zhang W. Thin-film sensing with planar terahertz metamaterials: sensitivity and limitations. Optics Express, 2008, 16(3): 1786–1795
28. Driscoll T, Andreev G O, Basov D N, Palit S, Cho S Y, Jokerst N M, Smith D R. Tuned permeability in terahertz split-ring resonators for devices and sensors. Applied Physics Letters, 2007, 91(6): 062511
29. Chen H T, Yang H, Singh R, O'Hara J F, Azad A K, Trugman S A, Jia Q X, Taylor A J. Tuning the resonance in high-temperature superconducting terahertz metamaterials. Physical Review Letters, 2010, 105(24): 247402
30. Katsarakis N, Konstantinidis G, Kostopoulos A, Penciu R S, Gundogdu T F, Kafesaki M, Economou E N, Koschny T, Soukoulis C M. Magnetic response of split-ring resonators in the far-infrared frequency regime. Optics Letters, 2005, 30(11): 1348–1350
31. Quan B G, Xu X L, Yang H F, Xia X X, Wang Q, Wang L, Gu C Z, Li C, Li F. Time-resolved broadband analysis of split ring resonators in terahertz region. Applied Physics Letters, 2006, 89 (4): 041101
32. Rockstuhl C, Lederer F, Etrich C, Zentgraf T, Kuhl J, Giessen H. On the reinterpretation of resonances in split-ring-resonators at normal incidence. Optics Express, 2006, 14(19): 8827–8836
33. Padilla W J, Taylor A J, Highstrete C, Lee M, Averitt R D. Dynamical electric and magnetic metamaterial response at terahertz frequencies. Physical Review Letters, 2006, 96(10): 107401
34. Driscoll T, Andreev G O, Basov D N, Palit S, Ren T, Mock J, Cho S Y, Jokerst N M, Smith D R. Quantitative investigation of a terahertz artificial magnetic resonance using oblique angle spectroscopy. Applied Physics Letters, 2007, 90(9): 092508
35. Padilla W J, Aronsson M T, Highstrete C, Lee M, Taylor A J, Averitt R D. Electrically resonant terahertz metamaterials: Theoretical and experimental investigations. Physical Review B, 2007, 75(4): 041102

36. Padilla W J. Group theoretical description of artificial electromagnetic metamaterials. Optics Express, 2007, 15(4): 1639–1646
37. O'Hara J F, Smirnova E, Azad A K, Chen H-T, Taylor A J. Effects of microstructure variations on macroscopic terahertz metafilm properties. Active and Passive Electronic Components, 2007, 2007: 49691
38. O'Hara J F, Smirnova E, Chen H T, Taylor A J, Averitt R D, Highstrete C, LeeM, PadillaW J. Properties of planar electric metamaterials for novel terahertz applications. Journal of Nanoelectronics and Optoelectronics, 2007, 2(1): 90–95
39. Azad A K, Taylor A J, Smirnova E, O'Hara J F. Characterization and analysis of terahertz metamaterials based on rectangular split-ring resonators. Applied Physics Letters, 2008, 92(1): 011119
40. Fedotov V A, Rose M, Prosvirnin S L, Papasimakis N, Zheludev N I. Sharp trapped-mode resonances in planar metamaterials with a broken structural symmetry. Physical Review Letters, 2007, 99 (14): 147401
41. Singh R, Al-Naib I A I, Koch M, Zhang W. Sharp Fano resonances in THz metamaterials. Optics Express, 2011, 19(7): 6312–6319
42. Munk B A. Frequency Selective Surfaces: Theory and Design. New York: John Wiley & Sons, 2000
43. Smith D R, Vier D C, Koschny T, Soukoulis C M. Electromagnetic parameter retrieval from inhomogeneous metamaterials. Physical Review E, 2005, 71(3): 036617
44. Holloway C L, Kuester E F, Gordon J A, O'Hara J, Booth J, Smith D R. An overview of the theory and applications of metasurfaces: the two-dimensional equivalents of metamaterials. IEEE Antennas and Propagation Magazine, 2012, 54(2): 10–35
45. Chen H T. Interference theory of metamaterial perfect absorbers. Optics Express, 2012, 20(7): 7165–7172
46. Landy N I, Sajuyigbe S, Mock J J, Smith D R, Padilla W J. Perfect metamaterial absorber. Physical Review Letters, 2008, 100(20): 207402
47. Tao H, Landy N I, Bingham C M, Zhang X, Averitt R D, Padilla W J. A metamaterial absorber for the terahertz regime: design, fabrication and characterization. Optics Express, 2008, 16(10): 7181–7188
48. Landy N I, Bingham C M, Tyler T, Jokerst N, Smith D R, Padilla W J. Design, theory, and measurement of a polarization-insensitive absorber for terahertz imaging. Physical Review B, 2009, 79(12): 125104
49. Tao H, Bingham C M, Strikwerda A C, Pilon D, Shrekenhamer D, Landy N I, Fan K, Zhang X, Padilla W J, Averitt R D. Highly flexible wide angle of incidence terahertz metamaterial absorber: design, fabrication, and characterization. Physical Review B, 2008, 78(24): 241103
50. Diem M, Koschny T, Soukoulis C M. Wide-angle perfect absorber/thermal emitter in the terahertz regime. Physical Review B, 2009, 79(3): 033101
51. Shchegolkov D Y, Azad A K, O'Hara J F, Simakov E I. Perfect subwavelength fishnetlike metamaterial-based film terahertz absorbers. Physical Review B, 2010, 82(20): 205117
52. Wen Q Y, Zhang H W, Xie Y S, Yang Q H, Liu Y L. Dual band terahertz metamaterial absorber: design, fabrication, and characterization. Applied Physics Letters, 2009, 95(24): 241111
53. Ye Y Q, Jin Y, He S L. Omnidirectional, polarization-insensitive and broadband thin absorber in the terahertz regime. Journal of the Optical Society of America. B, 2010, 27(3): 498–504
54. Tao H, Bingham C M, Pilon D, Fan K B, Strikwerda A C, Shrekenhamer D, Padilla W J, Zhang X, Averitt R D. A dual band terahertz metamaterial absorber. Journal of Physics. D, 2010, 43 (22): 225102
55. Shen X, Yang Y, Zang Y, Gu J, Han J, Zhang W, Cui T J. Triple-band terahertz metamaterial absorber: design, experiment, and physical interpretation. Applied Physics Letters, 2012, 101(15): 154102
56. Huang L, Chowdhury D R, Ramani S, Reiten M T, Luo S N, Taylor A J, Chen H T. Experimental demonstration of terahertz metamaterial absorbers with a broad and flat high absorption band. Optics Letters, 2012, 37(2): 154–156
57. Huang L, Chowdhury D R, Ramani S, Reiten M T, Luo S N, Azad A K, Taylor A J, Chen H T. Impact of resonator geometry and its coupling with ground plane on ultrathin metamaterial perfect absorbers. Applied Physics Letters, 2012, 101(10): 101102
58. Wen Q Y, Xie Y S, Zhang H W, Yang Q H, Li Y X, Liu Y L. Transmission line model and fields analysis of metamaterial absorber in the terahertz band. Optics Express, 2009, 17(22): 20256–20265
59. Chen H T, Zhou J, O'Hara J F, Chen F, AzadA K, TaylorA J. Antireflection coating using metamaterials and identification of its mechanism. Physical Review Letters, 2010, 105(7): 073901
60. Chen H T, Zhou J F, O'Hara J F, TaylorA J. A numerical investigation of metamaterial antireflection coatings. Terahertz Science and Technology, 2010, 3(2): 66–73
61. Strikwerda A C, Fan K, Tao H, Pilon D V, Zhang X, Averitt R D. Comparison of birefringent electric split-ring resonator and meanderline structures as quarter-wave plates at terahertz frequencies. Optics Express, 2009, 17(1): 136–149
62. Peralta X G, Smirnova E I, Azad A K, Chen H T, Taylor A J, Brener I, O'Hara J F. Metamaterials for THz polarimetric devices. Optics Express, 2009, 17(2): 773–783
63. Cong L Q, Cao W, Tian Z, Gu J Q, Han J G, Zhang W L. Manipulating polarization states of terahertz radiation using metamaterials. New Journal of Physics, 2012, 14(11): 115013
64. Zalkovskij M, Malureanu R, Kremers C, Chigrin D N, Novitsky A, Zhukovsky S, Tang P T, Jepsen P U, Lavrinenko A V. Optically active Babinet planar metamaterial film for terahertz polarization manipulation. Laser & Photonics Reviews, 2013, 7(5): 810–817
65. Markovich D L, Andryieuski A, Zalkovskij M, Malureanu R, Lavrinenko A V. Metamaterial polarization converter analysis: limits of performance. Applied Physics B, , 2013, 112(2): 143–152
66. Chiang Y J, Yen T J. A composite-metamaterial-based terahertz-wave polarization rotator with an ultrathin thickness, an excellent conversion ratio, and enhanced transmission. Applied Physics Letters, 2013, 102(1): 011129
67. Weis P, Paul O, Imhof C, Beigang R, Rahm M. Strongly birefringent metamaterials as negative index terahertz wave plates. Applied Physics Letters, 2009, 95(17): 171104
68. Yu N, Genevet P, Kats M A, Aieta F, Tetienne J P, Capasso F, Gaburro Z. Light propagation with phase discontinuities: generalized laws of reflection and refraction. Science, 2011, 334(6054): 333–337

69. Zhang X, Tian Z, Yue W, Gu J, Zhang S, Han J, Zhang W. Broadband terahertz wave deflection based on C-shape complex metamaterials with phase discontinuities. Advanced Materials, 2013, 25(33): 4567–4572
70. Neu J, Beigang R, Rahm M. Metamaterial-based gradient index beam steerers for terahertz radiation. Applied Physics Letters, 2013, 103(4): 041109
71. Grady N K, Heyes J E, Chowdhury D R, Zeng Y, Reiten M T, Azad A K, Taylor A J, Dalvit D A R, Chen H T. Terahertz metamaterials for linear polarization conversion and anomalous refraction. Science, 2013, 340(6138): 1304–1307
72. Cong L Q, Cao W, Zhang X Q, Tian Z, Gu J Q, Singh R, Han J G, Zhang W L. A perfect metamaterial polarization rotator. Applied Physics Letters, 2013, 103(17): 171107
73. Cong L Q, Xu N N, Gu J Q, Singh R, Han J G, Zhang W L. Highly flexible broadband terahertz metamaterial quarter-wave plate. Laser & Photonics Reviews, 2014: Early View
74. Hu D, Wang X K, Feng S F, Ye J S, Sun W F, Kan Q, Klar P J, Zhang Y. Ultrathin terahertz planar elements. Advanced Optical Materials, 2013, 1(2): 186–191
75. Jiang X Y, Ye J S, He J W, Wang X K, Hu D, Feng S F, Kan Q, Zhang Y. An ultrathin terahertz lens with axial long focal depth based on metasurfaces. Optics Express, 2013, 21(24): 30030–30038
76. Burckel D B, Wendt J R, Ten Eyck G A, Ginn J C, Ellis A R, Brener I, Sinclair M B. Micrometer-scale cubic unit cell 3D metamaterial layers. Advanced Materials, 2010, 22(44): 5053–5057
77. Randhawa J S, Gurbani S S, Keung M D, Demers D P, Leahy-Hoppa M R, Gracias D H. Three-dimensional surface current loops in terahertz responsive microarrays. Applied Physics Letters, 2010, 96(19): 191108
78. Soukoulis C M, Wegener M. Past achievements and future challenges in the development of three-dimensional photonic metamaterials. Nature Photonics, 2011, 5(9): 523–530
79. Moser H O, Rockstuhl C. 3D THz metamaterials from micro/nanomanufacturing. Laser & Photonics Reviews, 2012, 6(2): 219–244
80. Choi M, Lee S H, Kim Y, Kang S B, Shin J, Kwak M H, Kang K Y, Lee Y H, Park N, Min B. A terahertz metamaterial with unnaturally high refractive index. Nature, 2011, 470(7334): 369–373
81. Kadow C, Fleischer S B, Ibbetson J P, Bowers J E, Gossard A C, Dong J W, Palmstrom C J. Self-assembled ErAs islands in GaAs: Growth and subpicosecond carrier dynamics. Applied Physics Letters, 1999, 75(22): 3548–3550
82. Chen H T, Padilla W J, Zide J M O, Bank S R, Gossard A C, Taylor A J, Averitt R D. Ultrafast optical switching of terahertz metamaterials fabricated on ErAs/GaAs nanoisland superlattices. Optics Letters, 2007, 32(12): 1620–1622
83. Roy Chowdhury D, Singh R, O'Hara J F, Chen H T, TaylorA J, AzadA K. Dynamically reconfigurable terahertz metamaterial through photo-doped semiconductor. Applied Physics Letters, 2011, 99(23): 231101
84. Takano K, Shibuya K, Akiyama K, Nagashima T, Miyamaru F, Hangyo M. A metal-to-insulator transition in cut-wire-grid metamaterials in the terahertz region. Journal of Applied Physics, 2010, 107(2): 024907
85. Gu J, Singh R, Liu X, Zhang X, Ma Y, Zhang S, Maier S A, Tian Z, Azad A K, Chen H T, Taylor A J, Han J, Zhang W. Active control of electromagnetically induced transparency analogue in terahertz metamaterials. Nature Communications, 2012, 3: 1151
86. Roy Chowdhury D, Singh R, Taylor A J, Chen H T, Azad A K. Ultrafast manipulation of near field coupling between bright and dark modes in terahertz metamaterial. Applied Physics Letters, 2013, 102(1): 011122
87. Chen H T, O'Hara J F, Azad A K, Taylor A J, Averitt R D, ShrekenhamerD B, PadillaW J. Experimental demonstration of frequency-agile terahertz metamaterials. Nature Photonics, 2008, 2 (5): 295–298
88. Shen N H, Kafesaki M, Koschny T, Zhang L, Economou E N, Soukoulis C M. Broadband blueshift tunable metamaterials and dual-band switches. Physical Review B, 2009, 79(16): 161102
89. Shen N H, Massaouti M, Gokkavas M, Manceau J M, Ozbay E, Kafesaki M, Koschny T, Tzortzakis S, Soukoulis C M. Optically implemented broadband blueshift switch in the terahertz regime. Physical Review Letters, 2011, 106(3): 037403
90. Zhang S, Zhou J, Park Y S, Rho J, Singh R, Nam S, Azad A K, Chen H T, Yin X, Taylor A J, Zhang X. Photoinduced handedness switching in terahertz chiral metamolecules. Nature Communications, 2012, 3: 942
91. Zhang S, Park Y S, Li J, Lu X, Zhang W, Zhang X. Negative refractive index in chiral metamaterials. Physical Review Letters, 2009, 102(2): 023901
92. Zhou J F, Chowdhury D R, Zhao R K, Azad A K, Chen H T, Soukoulis C M, Taylor A J, O'Hara J F. Terahertz chiral metamaterials with giant and dynamically tunable optical activity. Physical Review B, 2012, 86(3): 035448
93. Fan K B, Zhao X G, Zhang J D, Geng K, Keiser G R, Seren H R, Metcalfe G D, Wraback M, Zhang X, Averitt R D. Optically tunable terahertz metamaterials on highly flexible substrates. IEEE Transactions on Terahertz Science and Technology, 2013, 3(6): 702–708
94. Chen H T, Padilla W J, Zide J M O, Gossard A C, Taylor A J, Averitt R D. Active terahertz metamaterial devices. Nature, 2006, 444(7119): 597–600
95. Chen H T, Padilla W J, Cich M J, Azad A K, Averitt R D, Taylor A J. A metamaterial solid-state terahertz phase modulator. Nature Photonics, 2009, 3(3): 148–151
96. Chen H T, Palit S, Tyler T, Bingham C M, Zide J M O, O'Hara J F, Smith D R, Gossard A C, Averitt R D, Padilla W J, JokerstN M, TaylorA J. Hybrid metamaterials enable fast electrical modulation of freely propagating terahertz waves. Applied Physics Letters, 2008, 93(9): 091117
97. Shrekenhamer D, Rout S, Strikwerda A C, Bingham C, Averitt R D, Sonkusale S, Padilla W J. High speed terahertz modulation from metamaterials with embedded high electron mobility transistors. Optics Express, 2011, 19(10): 9968–9975
98. Chen H T, Lu H, Azad A K, Averitt R D, Gossard A C, Trugman S A, O'Hara J F, Taylor A J. Electronic control of extraordinary terahertz transmission through subwavelength metal hole arrays. Optics Express, 2008, 16(11): 7641–7648
99. Paul O, Imhof C, Lägel B, Wolff S, Heinrich J, Höfling S, Forchel

A, Zengerle R, Beigang R, Rahm M. Polarization-independent active metamaterial for high-frequency terahertz modulation. Optics Express, 2009, 17(2): 819–827

100. Peralta X G, Brener I, Padilla W J, Young E W, Hoffman A J, Cich M J, Averitt R D, Wanke M C, Wright J B, Chen H T, O'Hara J F, Taylor A J, Waldman J, Goodhue W D, LiJ, RenoJ. External modulators for terahertz quantum cascade lasers based on electrically-driven active metamaterials. Metamaterials, 2010, 4 (2–3): 83–88
101. Chan W L, Chen H T, Taylor A J, Brener I, Cich M J, Mittleman D M. A spatial light modulator for terahertz beams. Applied Physics Letters, 2009, 94(21): 213511
102. Shrekenhamer D, Montoya J, Krishna S, Padilla W J. Four-color metamaterial absorber THz spatial light modulator. Advanced Optical Materials, 2013, 1(12): 905–909
103. Karl N, Reichel K, Chen H T, Taylor A J, Brener I, Benz A, Reno J L, Mendis R, Mittleman D M. An electrically driven terahertz metamaterial diffractive modulator with more than 20 dB of dynamic range. Applied Physics Letters, 2014, 104(9): 091115
104. Fan K, Hwang H Y, Liu M, Strikwerda A C, Sternbach A, Zhang J, Zhao X, Zhang X, Nelson K A, Averitt R D. Nonlinear terahertz metamaterials via field-enhanced carrier dynamics in GaAs. Physical Review Letters, 2013, 110(21): 217404
105. Scalari G, Maissen C, Turcinková D, Hagenmüller D, De Liberato S, Ciuti C, Reichl C, Schuh D, Wegscheider W, Beck M, Faist J. Ultrastrong coupling of the cyclotron transition of a 2D electron gas to a THz metamaterial. Science, 2012, 335(6074): 1323–1326

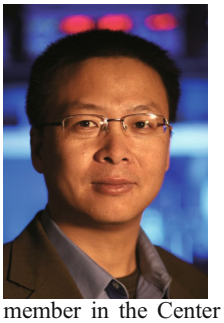

Hou-Tong Chen received his B.S. and M.S. degrees from the University of Science and Technology of China in 1997 and 2000, respectively, and Ph.D degree from Rensselaer Polytechnic Institute in 2004, all in physics. Between 05/2005 and 05/2008, he was a postdoctoral research associate in Los Alamos National Laboratory (LANL). Since 06/2008, he has been a technical staff member in the Center for Integrated Nanotechnologies (CINT) at LANL, a Department of Energy/Office of Science Nanoscale Science Research Center (NSRC) jointly operated by Los Alamos and Sandia National Laboratories as a national user facility. His research interests are in metamaterials and terahertz science and technology. He has co-authored over 50 publications in peer-reviewed journals including *Science, Nature, Nature Photonics,* and *Physical Review Letters,* which have been totally cited over 2400 times according to ISI Web of Science. He has delivered over 50 invited presentations in international conferences as well as colloquia and seminars in research institutions. He received LANL Achievement Awards in 2013 and 2007. He has been serving as a member of the Editorial Committee in *Scientific Reports, International Journal of Terahertz Science and Technology* and *Frontiers of Optoelectronics.* He also served many conferences and workshops in the organizing committee, advisory committee, or technical program committee.